

## 14.3: Electronic interface Modules for Solid-State Chemical Sensors

Sam McKennoch, Denise M. Wilson

Department of Electrical Engineering, University of Washington,  
Seattle WA 98195-2500

skennoch@u.washington.edu denisew@u.washington.edu

### Abstract

*Plug and play modules for interfacing three common types of solid-state chemical sensors are presented. The self-contained (integrated circuit) modules detect a baseline signal from a sensor and auto-zero the signal to compensate for baseline variations, both immediately after fabrication and periodically during the lifetime of the sensor. The signal compensation technique is based on the governing transduction principles of the chemical sensor, thereby enabling signals to be compensated without distortion. After fabrication, sensors are auto-zeroed at their field operating conditions to ensure that all homogenous sensors begin at the same baseline output. Re-zeroing is completed at a time scale compatible with the drift and lifetime of the sensor and is automated in similar manner to the initial autozeroing step that occurs during calibration. The matching of automated baseline compensation to governing transduction principles for chemical sensors is a novel effort. This paper will present experimental results at the circuit, architecture and system level using chemFETs, composite film polymer chemiresistors and tin-oxide chemiresistors. In typical experiments, the described circuit exhibits half the response time to low concentrations of chemicals and over an 11% improvement in analyte discriminating ability versus uncompensated sensors.*

### INTRODUCTION

Variable sensor baseline is a major issue that affects chemical sensor performance. The baseline refers to the response of the sensor when there is no chemical analyte present. For example, in the case of composite film polymer chemiresistors, the baseline is manifested as the (unstimulated) sensor resistance. The resistance of composite film polymer chemiresistors has been measured in our laboratory to vary from 25k $\Omega$  to 300k $\Omega$ . This initial, wide baseline variation is compounded by sensor drift over time and other aging factors.

Drift can be caused in part by the incomplete release of analyte vapor after an experiment has ended. Drift rates noted in experiments by the authors are generally limited to a 3% percent increase from the original baseline value over the period of a week. In experiments done elsewhere on com-

posite film polymer chemiresistors, drift rates of approximately 16% were observed over a 3 month period. Drift does not strongly affect the sensor sensitivity and if compensated, will have only a negligible effect [1]. Because the rate of chemical sensor drift in general is much slower than the rate of chemical sensor reaction to an analyte, a baseline compensator need only recompensate the sensor periodically to maintain a near-constant baseline value in the absence of an analyte. This recompensation can be done in real-time using a baseline compensator circuit. Compensation changes the problem to one of optimizing the drift reset frequency in the software, which is easily changed to accommodate a wide variety of situations. Drift compensation further limits and standardizes sensor dynamic range, thereby preventing a loss in system resolution due to drift.

A handful of research efforts have demonstrated techniques for improving portable instrument viability by reducing the inherent variation in chemical sensors with baseline compensation techniques. Apsel *et al* uses an adaptive, programmable amplifier to stabilize chemiresistors at a predetermined baseline value using floating gate analog memory and novel filtering techniques. The floating gate capability allows a continuous range of programmable values, theoretically enabling perfect baseline compensation (within the constraints of transistor performance); however, these circuits also contribute distortion to the sensor response, generating different response curves for the same analyte, same type of sensor, but different baseline resistances [2]. Using a different circuit design approach, Neves and Hatfield have constructed an ASIC specifically designed to extract response signals from an array of polymer chemiresistors. This circuit results in fundamental distortion of the sensor signal by creating a non-linear response of the output current in relation to the input concentration. The ASIC is a versatile generic module for sensor resistance preprocessing, but contains bulky amplifiers and multipliers that may limit usefulness for large arrays in portable instruments in terms of space and power consumption [3].

The authors have also previously demonstrated a discrete version of this compensation circuit [4]. Advantages of the present integrated design over the discrete circuit include

size (a factor of 1310 in reduced volume), cost (a factor of over 40 in reduced cost per compensated sensor), and accuracy.

This paper presents a mixed signal method for sourcing a constant current through a chemiresistor or chemFET in such a way that the sensor response is not distorted during compensation. This circuit is the first in a series of integrated baseline circuits for different chemical sensor technologies that provides modular baseline-independent compensation with no distortion of chemical sensor signal.

## SENSOR BACKGROUND AND APPLICATION

### Composite Film Polymer Chemiresistors

Composite film polymer chemiresistors are made of an insulating polymer matrix implanted with conductive particles of carbon-black [5]. As the sensor is exposed to an analyte to which it is sensitive, the polymer swells. This swelling causes the conductive carbon-black particles to move farther apart, thereby changing the conductivity of the sensor. Large amounts of swelling produce a non-linear relationship with concentration, however for typical small-signal use, these sensors demonstrate a linear response [6]:

$$\frac{\Delta R}{R_o} = k[C] \quad (1)$$

$R_o$  is the baseline resistance of the sensor;  $\Delta R$  is the change in resistance from the baseline value;  $[C]$  is the concentration of the analyte, typically in ppm; and  $k$  is a sensor constant. This equation demonstrates that the slope of the response curve is not affected by the baseline value of resistance.  $k$  at least in part depends on the chemical applied and the type of polymer being used.

If one were to measure the resistance of the sensor directly, equation (1) changes to:

$$R = R_o + R_o k[C] \quad (2)$$

Baseline compensation establishes the initial output baseline voltage,  $V_b$ , at a constant value for all sensors, regardless of the initial baseline resistance. It achieves this result by use of a variable current source,  $I_{Set}$ . After baseline compensation, the input-output equation for composite film polymer chemiresistors then changes to:

$$V_o = I_{Set}R = I_{Set}R_o \left(1 + \frac{\Delta R}{R_o}\right) = V_b(1 + k[C]) \quad (3)$$

From the above equation, at zero analyte concentration, the output voltage is set to a desired baseline voltage, thereby reducing sensor variation by compensating for the arbitrary

baseline resistance. The linear transformation also preserves the sensor response shape (low distortion). Drift is compensated at appropriate times in the sensor lifetime by re-zeroing each sensor to the predetermined uniform baseline state.

### Tin-Oxide Chemiresistors

Another type of chemiresistor is the Tin-Oxide sensor. Tin-Oxide is an n-type semiconducting metal oxide whose conductivity properties are highly sensitive to gases present in the environment. Oxygen species in the thin film that make up the sensor build dangling bonds and other lattice vacancies. Reducing gases in the environment combine with oxygen in the thin film to enable the change in sensor conductivity and resistance[7],[8]. Using a necessary heating element, the tin-oxide sensors' resistance can be measured as a response to certain types of gases. The input-output equation may be stated as below:

$$\frac{1}{R} = \frac{1}{R_o} + a[C]^r \quad (4)$$

$a$  is a sensitivity coefficient.  $r$  is a power law exponent for oxides. A strong dependence on temperature and humidity has further been observed and characterized [7],[8]. As with the composite film polymer chemiresistors the signal response for the tin-oxide sensors is not distorted. However, concentration is now linear with the natural log of sensor resistance, and so this new relationship must be taken into account when using homogenous arrays of these sensors.

### ChemFETs

One type of FET based chemical sensor is the ChemFET. ChemFETs are Chemically Sensitive Field Effect Transistors. They are inexpensive and easy to integrate into support circuitry. ChemFETs are built with a chemically sensitive gate material (generally a heavily-doped conducting polymer) applied on the gate oxide. When a chemical is applied to which the gate material is sensitive, the fermi level at the gate shifts causing a change in the work function of the metal via bulk and surface modulation thereby causing the threshold voltage of the FET to change in a measurable way [9],[10]. Although research continues to acquire a more precise definition, at this time the input-output relationship of a diode-connected ChemFET in the saturation region of operation with a constant drain-source current applied can be modelled as:

$$V_o = x_0 \ln(a[C]) + x_1 + \sqrt{\frac{2I_D}{k(W/L)}} \quad (5)$$

$x_0$  and  $x_1$  are constants which depend on physical device parameters associated with the materials used to build the

ChemFET and the geometry of the device as well. They do not change in a meaningful way in response to an applied analyte and can be determined empirically.  $a$  is a scaling factor.  $[C]$  is the concentration of the analyte.  $I_D$  is the drain current through the ChemFET. It is generally set to some constant value.  $k'$  is another physical parameter.  $W$  and  $L$  are the width and length of the FET channel. The nature of the input-output equation is then logarithmic. However, this formula is only valid for moderate concentration ranges [10].

### CIRCUIT DESCRIPTION

A block diagram of the auto-zeroing baseline compensation scheme is shown in Figure 1. Compensation begins when the system is reset, setting the counter output to zero. The first stage is then externally enabled by bringing both the write-select line on Memory 1 and the Counter enable high. These actions cause Digital to Analog Converter (DAC) 1 to receive four-bit binary inputs that are counting up. DAC 1 converts this digital nibble to an analog current. The range of the current is set by an external reference,  $I_{ref1}$ , in order to provide flexibility in compensating a wide range of initial sensor states. Eventually, the current injected into the sensor will generate a voltage larger than the desired baseline voltage causing the output of the comparator to go from high to low. The write-select line on Memory 1 is then set low, the Counter reset, and the Memory 2 line set high, thereby enabling stage 2 to begin.

Although external pins provide nearly infinite resolution in setting the bias currents, one possible scheme for setting the bias current of stage 2 follows. In stage 2, the second DAC is biased at a current that is approximately 1/15th that of the first stage. The current from the second DAC is subtracted

from that of the first DAC, thereby decreasing the output voltage (by a fraction of the step size in stage 1) as the counter counts up until the comparator again changes states. The final reference current for the second DAC is subsequently switched from 1/15th to 1/16th that of the first stage in order to produce a zero average quantization error from baseline. The DAC is divided into two 4-bit stages to avoid using the large amount of real estate on a single 8-bit DAC and an 8-bit counter. The following equations govern the final baseline voltage:

$$V_b = I_{ref} R_s \left( n_1 - \frac{n_2}{16} \right) \quad (6)$$

$$n_1 = \left\lceil \frac{V_{db}}{I_{ref} R_s} \right\rceil \quad (7)$$

$$n_2 = \left\lceil \frac{15(I_{ref} n_1 R_s - V_{db})}{I_{ref} R_s} \right\rceil \quad (8)$$

$V_b$  is the actual compensated baseline voltage;  $I_{ref}$  is the reference current for DAC 1;  $R_s$  is the sensor resistance; and  $V_{db}$  is the desired baseline voltage. Average error across homogenous sensor arrays should be equal to zero to ensure uniformity in consideration of sensor signals in subsequent signal processing. Figure 2 shows the quantization error produced in compensating a wide range of baseline resistance values, assuming that the minimum value to be detected is  $25k\Omega$ . (a) represents the quantization error for an 8-bit DAC used with baseline resistances ranging from  $25k\Omega$  to  $300k\Omega$  and  $V_{db} = 2V$ . The 8-bit error range and mean are  $94.6$  mV and  $2.026$  V respectively. (b) represents

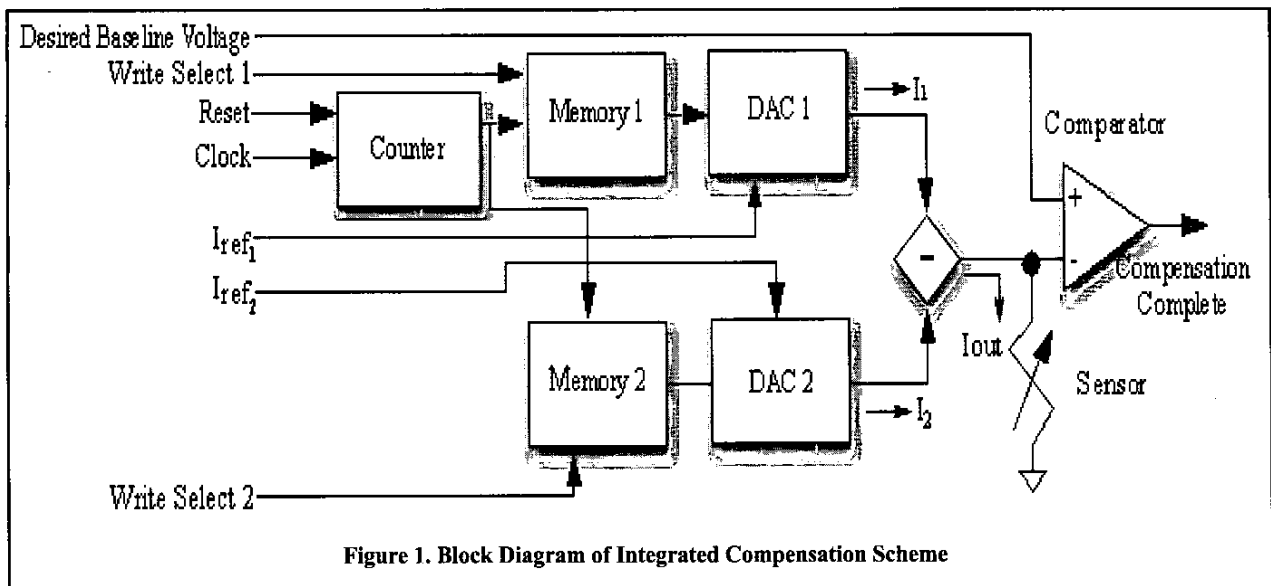
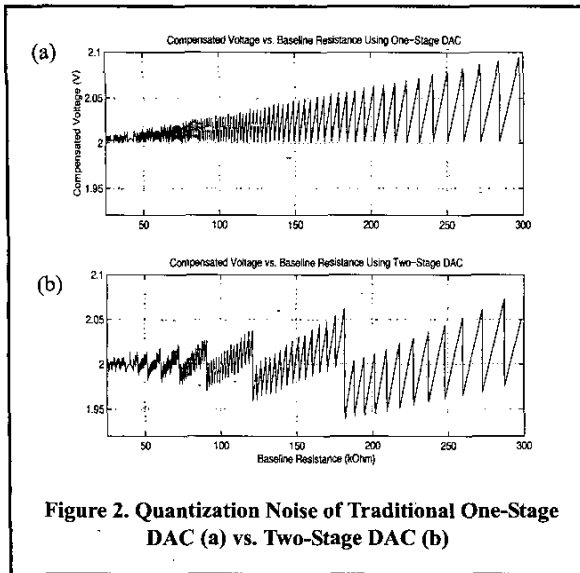


Figure 1. Block Diagram of Integrated Compensation Scheme



**Figure 2. Quantization Noise of Traditional One-Stage DAC (a) vs. Two-Stage DAC (b)**

the quantization error if a two-stage (4-bits per stage) DAC was used, also with  $V_{db} = 2V$ . The two stage error range and mean are 132.6 mV and 2.001 V respectively. Schematics of key circuit components to the baseline compensator are shown in Figure 3. All current mirrors are cascode current mirrors for high output impedance. Refer to Figure 1 for signal explanation in the context of the system block diagram

### EXPERIMENTAL RESULTS

The compensation circuit has been fabricated using an AMI  $1.5\mu\text{m}$  n-well process through MOSIS. The available die size is 2.2mm by 2.2mm. Circuit, system, and architecture level results are described below.

#### Circuit Level Results

Simulated results showing the compensation process and the effect of baseline compensation on sensor response are shown in Figure 4 and Figure 5 respectively. In Figure 4, initial compensation (DAC 1) runs from data point 0 to 10.

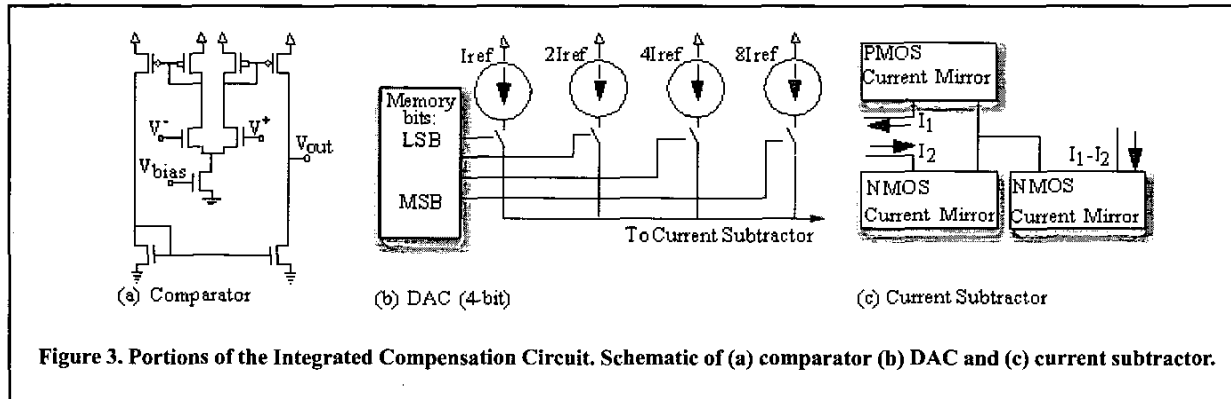


**Figure 3. Portions of the Integrated Compensation Circuit. Schematic of (a) comparator (b) DAC and (c) current subtractor.**

Final compensation (DAC 2) is performed from data point 15 to 25. Zero average error compensation (reference current switch) occurs at data point 29. The comparator changes states to reflect the compensation stage.

In Figure 5, uncompensated values in (a) are generated using a constant  $50\mu\text{A}$  current source with baseline resistances of  $25\text{k}\Omega$  to  $300\text{k}\Omega$ . The minimum detectable non-compensated resistance change is  $81.8\Omega$  (0.327% to 0.027% of baseline). When using compensation in (b), the minimum detectable change for  $25\text{k}\Omega$  to  $300\text{k}\Omega$  sensor resistances range from  $1.2\Omega$  to  $14.6\Omega$  (0.010%) respectively, produced from a voltage range of 2 to 2.4V. Without compensation, an ADC with more than 18-bits would be needed to accomplish the same performance as a 12-bit ADC with baseline compensated sensors. Compensation provides up to a factor of 68 improvement in response in this example. The minimum detectable change in concentration of cyclohexane for the non-compensated circuit is as high as 16.4 ppm, while for any of the compensated sensors, the minimum detectable concentration change is 0.25 ppm (a significant improvement in detection threshold).

Expected performance measurements are verified with experimental results. In the case of chemiresistors, varying the sensor resistance by up to 50% from the baseline resistance resulted in an output voltage error from the expected output voltage of less than 1%. This result shows that the circuit is capable of holding a constant output current under circumstances of highly variant loading conditions.

Using a  $100\text{k}\Omega$  chemiresistor, the compensation circuit is used to compensate the output voltage to various values from 1 to 3 V. Using a single stage, error between the desired baseline voltage and the measured baseline voltage averages 10%. Using both stages, the error is reduced to under 0.5%.

Two drift tests are performed on the integrated circuit. First, it is desired to make certain that the constant output current would not drift over time. A fixed value resistor was attached to the circuit output and compensated to

2.013V. Measurements taken at as much as 24 hours later show that output voltage remains within 2mV of the original compensated value.

The second part of the drift test is designed to verify that a sensor which had drifted from its baseline value, not in response to any analyte could be recompensated. The typical result shown in Figure 6 demonstrates that indeed drift compensation is possible. The recompensated value was only 0.03% different from the original baseline voltage.

### Architecture Level Results

Figure 7 shows the measured error in compensating chemiresistors of varying baseline resistances to a baseline voltage of 2V for both one and two stages. The bias current for the second stage is set at 1/16 that of the first stage. In this case the circuit is calibrated to be able to compensate a minimum resistance of 25kΩ, typical of tin-oxide chemiresistors. As the baseline resistance deviates from this value, the baseline compensation error increases. Accurate compensation is possible for a wide range of baseline resistance, but accuracy increases as the possible resistance range is better understood. In the case of ChemFETs, the

output dynamic range, and therefore the concentration detection resolution is also reduced as follows. By examining the governing transduction mechanism equation (5), adjusting the bias current has the effect of adjusting the y-intercept of the response in such a way that all chemFETs respond in a similar voltage range. If the bias voltages that act to set the reference currents are tabulated for known sensor technologies, it becomes possible to use this compensation circuit in a plug and play manner to improve system concentration resolution and linearity.

### System Level Results

The simulated results previously presented in Figure 5 demonstrate the improvement in analyte detection resolution that is possible with this compensation circuit. In an experiment along the same lines as the simulation in Figure 5, two composite film polymer chemiresistors, one compensated and one uncompensated, are used to determine which of the sensors will first respond to an analyte. The analyte is placed in an open jar two feet from the sensors. One sensor is paired with a 50kΩ divider resistor for readout. The other sensor is placed in the compensation circuit. Using a

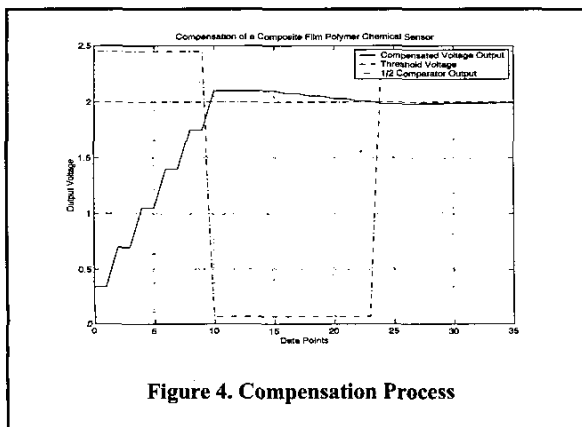


Figure 4. Compensation Process

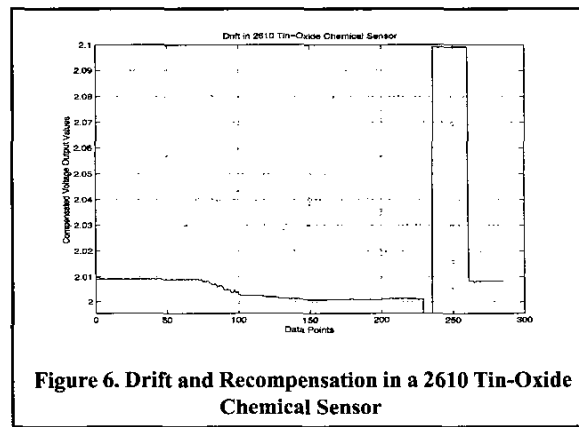


Figure 6. Drift and Recompensation in a 2610 Tin-Oxide Chemical Sensor

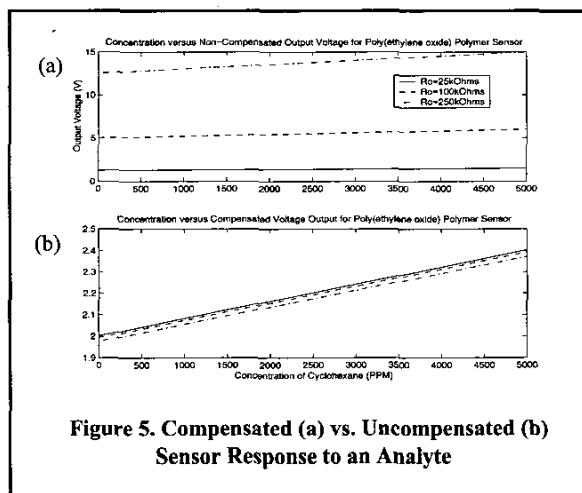


Figure 5. Compensated (a) vs. Uncompensated (b) Sensor Response to an Analyte

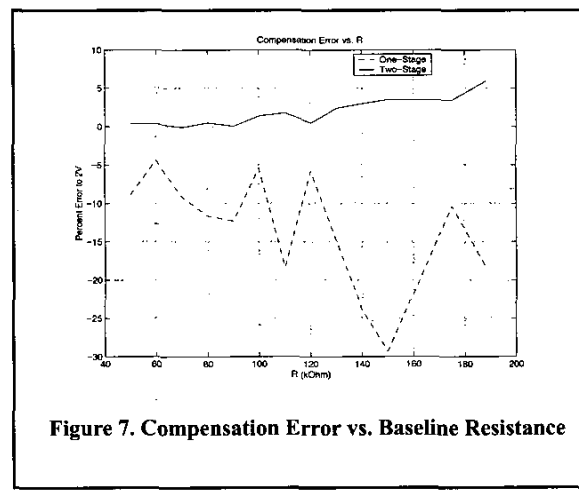


Figure 7. Compensation Error vs. Baseline Resistance

standard 12-bit data acquisition card, the minimum detectable voltage is 1.2mV. The compensated circuit detects the analyte after 20 seconds, while the non-compensated circuit took over twice as long. The compensated circuit demonstrates over twice the resolution for concentration detection in this experiment

Figure 8 demonstrates the results of principal component analysis, used here for analyte classification purposes. Data is taken using three different types of composite film polymer chemiresistors. The sensors are placed in a sealed chamber into which the analyte is allowed to diffuse. Measurements continued until the sensors reach a steady-state response. The figure shows the euclidean distance between the two-dimensional principal component transformed data for responses to Methanol and Ammonia. In this typical response the compensated sensors show an 11% improvement discriminating ability.

#### Future Work

The next version of the compensation circuit is currently being fabricated using an AMI 1.5 $\mu$ m n-well process through MOSIS. The available die size is 2.2mm by 2.2mm. While the original integrated circuit contained only one compensation circuit, the new version contains four. Using the current design, there is room on the available die for as many as 16 compensation circuits. However, the current need for output testing pins limit the number of integrated compensation circuits possible. Also included on the new integrated chip is a biologically-inspired circuit capable of performing cross-inhibition and cross-excitation between sensor responses. The ability to cross-inhibit and cross-excite will increase the ability of the circuit to preferentially detect analytes in the presence of interferents.

#### ACKNOWLEDGEMENTS

The authors would like to thank Nathan Lewis at the California Institute of Technology for providing composite polymer sensors and related data sets and Jiri Janata at the

Georgia Institute of Technology for providing chemFETs. We would also like to acknowledge the National Science Foundation (Award Number ECS-9996263 and ECS-9988905) for its support of this project.

#### CONCLUSION

We have successfully demonstrated the ability to compensate for variation in baseline of typical chemiresistors and chemFETs. The integrated circuit used to perform this compensation is capable of interacting with these different chemical sensors in a plug and play manner. Typical results indicate a 68-fold improvement in sensor signal resolution for a 12-bit A/D converter over its uncompensated counterpart. Compensation occurs without the distortion of the sensor response, a critical aspect of any electronic interface to sensor systems. Compensation for low-frequency drift has also been demonstrated.

#### REFERENCES

- [1] Mark C. Lonergan, Erik J. Severin, Brett J. Doleman, Sara A. Beaber, Robert H. Grubbs, and Nathan S. Lewis, "Array-Based Vapor Sensing Using Chemically Sensitive, Carbon-Black-Polymer Resistors," *Chemistry of Materials* **8**, No. 9, pp. 2298-2312, 1996.
- [2] Alyssa Apsel, Theron Stanford and Paul Hasler, "An Adaptive Front End for Olfaction," *ISCAS '98, Proceedings of the 1998 IEEE International Symposium on Circuits and Systems* **3**, pp. 107-110, 1998.
- [3] J. V. Hatfield and P. I. Neaves, "A Signal Processing ASIC for an Electronic Nose," *IEE Colloquium on Application Specific Integrated Circuits for Measurement Systems*, pp. 8/1 -8/5, 1994.
- [4] Sam McKennoch and Denise Wilson, "Autoranging Compensation for Variable Baseline Chemical Sensors," *Proceedings of the SPIE International Symposium on Environmental and Industrial Sensing*: Boston, MA, 2001.
- [5] Beth C. Muñoz et al., "Conductive polymer-carbon black composites-based sensor arrays for use in an electronic nose," *Sensor Review* **19**, No. 4, pp. 300-305, 1999.
- [6] Brett J. Doleman, Mark C. Lonergan, Erik J. Severin, Thomas P. Vaid, and Nathan S. Lewis, "Quantitative Study of the Resolving Power of Arrays of Carbon Black-Polymer Composites in Various-Sensing Tasks," *Analytical Chemistry* **70**, pp. 4177-4190, 1998.
- [7] Kousuke Ihokura and Joseph Watson, *The Stannic Oxide Gas Sensor*, pp. 49-88, CRC Press, Ann Arbor, 1994.
- [8] E. Llobet et. al, "Electrical equivalent models of semiconductor gas sensors using PSPICE," *Sensors and Actuators B* **77** pp. 275-280, 2001.
- [9] Jiri Janata and Robert J. Huber, *Principles of Chemical Sensors*, pp. 152-174, Academic Press, New York, 1985.
- [10] J. Janata, M. Josowicz, "Chemical Modulation of Work Function as a Transduction Mechanism for Chemical Sensors," *Accounts of Chemical Research* **31**, No. 5, pp. 241-248, 1998.

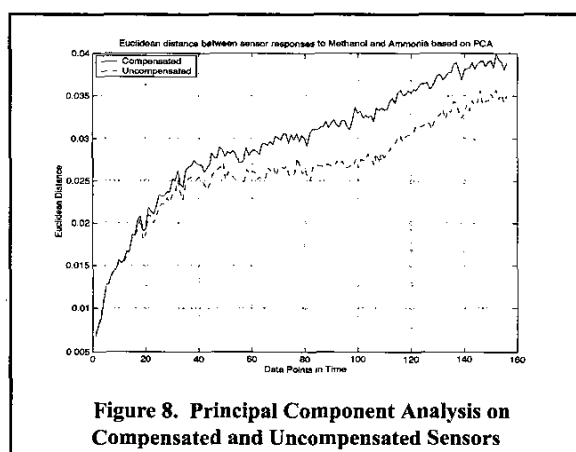


Figure 8. Principal Component Analysis on Compensated and Uncompensated Sensors